Supplementary material for: Stronger carbon uptake in eddy-resolving simulations of global warming

*Damien Couespel[a], Marina Lévy[a], Laurent Bopp [b]

[a]Sorbonne Université, LOCEAN-IPSL, CNRS/IRD/MNHN, Paris, France

[b]LMD-IPSL, École Normale Supérieure/PSL University, CNRS, École Polytechnique, Sorbonne Université, Paris, France

*Corresponding author: damien.couespel@locean-ipsl.upmc.fr

S1 About the models, configurations and experimental designs

Table S1 summarize the most important features of the models and configurations used in the study.

Horizontal resolution	**1° or 106 km**	**1/9° or 11.8 km**	**1/27° or 3.9 km**
Grid cell number	30×30	270×270	810×810
Time step	30 min	16 min	5 to 4.5 min
Number of CPU	1	64	800
CPU time (cpu. $\times$ real time)	20 min/simulated year	260 h/simulated year	7000 h/simulated year
Momentum diffusion	Horizontal laplacian	None	None
Viscosity coef.	10^5 m^{2}s^{-1}	None	None
Tracer advection scheme	TVD	MUSCL	MUSCL
Tracer diffusion	Isopycnal laplacian	None	Horizontal bilaplacian
$\mathbf{k}_{iso}$	500, 1000, 2000 m^{2}s^{-1}	None	-10^9 m^{4}s
$\mathbf{k}_{gm}$	500, 1000, 2000 m^{2}s^{-1}	None	None

Table S1. Resolution-dependent model features and parameters. For details on numerical schemes, see Madec et al. [2017] and Lévy et al. [2001]. Note that we added a minimum level of bilaplacian tracer diffusivity at 1/27° to insure numerical stability, and this was not needed at 1/9° resolution. This bilaplacian diffusion acts on the horizontal, unlike the laplacian diffusion acting along isopycnals in the 1° resolution simulations.

The biogeochemical model LOBSTER [Lévy et al., 2012, 2005] is a nitrogen cycle based model. A carbon cycle is activated (Tab S2). Carbon is exchanged with the atmosphere following gas exchange from Wanninkhof [1992, Eq. 8]. Dissolved inorganic carbon is consumed by (new and regenerated) primary production and produced during ammonium formation (Eq. 1). Alkalinity increases during ammonium formation and nitrate consumption (new production) and decreases during ammonium consumption (regenerated production) (Eq. 2). The carbon cycle does not take into account calcium carbonate ($CaCO_3$). Note that contrary to ESMs, here atmospheric CO_2 is not radiatively active. It is not related to temperature changes, i.e. atmospheric temperature and atmospheric CO_2 are two independent forcings of the model. This is convenient for conducting the different simulations.

For scarce of computation time, we have not run 4 simulations (CTL, BGC, RAD and COU) for each resolution. Instead, a second carbon cycle has been implemented in the model. The source and sink equations of this second carbon cycle are very similar, the same as the first carbon cycle. They only differ in the handling of the air-sea carbon flux. The first carbon cycle kept the atmospheric pCO_2 constant overtime, whereas the second carbon cycle increase the pCO_2 to simulate the release of carbon into the atmosphere by human activities. Thus, this second carbon cycle contains both natural and anthropogenic carbon, while the first cycle only contains natural carbon. Only 2 simulations have then been effectively run: with or without temperature increase. The first carbon cycle without temperature increase is the CTL simulation, the second carbon cycle without temperature increase is the BGC simulation, the first carbon cycle with the temperature increase is the RAD simulation and the second carbon cycle with temperature increase is the COU simulation.

$$S(DIC) = \overbrace{R_{C:N}\alpha_p\gamma \times (NP+RP)}^{\text{exsudation}} + \overbrace{R_{C:N}\alpha_z\tau_z \times ZOO}^{\text{excretion}} + \overbrace{R^{dom}_{C:N}\tau_{dom} \times DOM}^{\text{remineralization}} + fCO_2 - \overbrace{R_{C:N} \times (NP+RP)}^{\text{primary production}} \quad \textbf{Equation 1.}$$

$$S(ALK) = \overbrace{\tau_{dom} \times DOM + \alpha_z\tau_z \times ZOO + \alpha_p\gamma \times (NP+RP)}^{\text{ammonium formation}} - RP + NP \quad \textbf{Equation 2.}$$

DIC: dissolved inorganic carbon concentration [mol C m^{-3}], ALK: alkalinity concentration [mol m^{-3}], NP: new production [mol N m^{-3} s^{-1}], RP: regenerated production [mol N m^{-3} s^{-1}], ZOO: zooplankton concentration [mol N m^{-3}], DOM: dissolved organic matter concentration [mol N m^{-3}], fCO_2: air-sea flux [mol C m^{-3} s^{-1}]

$R_{C:N} = 6.56$ mol C mol N^{-1}, $R^{dom}_{C:N} = 12$ mol C mol N^{-1}, $\gamma = 0.05$, $\alpha_p = 0.75$, $\alpha_z = 0.7$, $\tau_z = 8.1e^{-7}$ s^{-1}, $\tau_{dom} = 6.43e^{-8}$ s^{-1}

Table S2. Carbon cycle equations and parameters. The two carbon cycle activated in the model have similar equations. They only differ in the computation of the air-sea carbon flux (fCO_2).

S2 About the carbon budgets

To have a finer understanding of the DIC budget, the upper and lower ocean have been divided in 3 boxes, the subtropical gyre boxes (STG), subpolar gyre boxes (SPG) and convection zone boxes (CZ), leading to 6 boxes in total. The DIC budget have been computed in these 6 boxes (Fig. S1). In addition, the advection term has been split in its different horizontal and vertical component using the yearly means of velocities and DIC. This give us some insight about the direction of the advective fluxes. However, because of the use of yearly means for computing the advective fluxes, the sum of the advective fluxes entering/exiting the boxes $\int_0^{70} \oint \vec{u} \cdot DIC \, \mathrm{ds\,dt}$ is not equal to the volume integral of the divergence of the advective fluxes $\int\int\int \vec{\nabla} \cdot (\vec{u} \cdot DIC) \, \mathrm{dx\,dy\,dz}$, the latter having been computed at each time step of the simulations.

Note that, because of a mishandling in the simulations outputs, the years 66 to 68 of the advection, diffusion and biological terms of the DIC budget have been lost for the COU simulation at 1/27° resolution. These missing years have been replaced by a linear interpolation between the years 65 to 69. This flaw only applies to the numbers for 1/27° resolution in figure S1b. Overall, the results from the 1/27° simulations are relatively close to the 1/9° simulations results. Then, our main conclusions, based on the difference between the coarse 1° simulations and the finer simulations, should not be affected.

References

Gurvan Madec, Romain Bourdallé-Badie, Pierre-Antoine Bouttier, Clément Bricaud, Diego Bruciaferri, Daley Calvert, Jérôme Chanut, Emanuela Clementi, Andrew Coward, Damiano Delrosso, Christian Ethé, Simona Flavoni, Tim Graham, James Harle, Doroteaciro Iovino, Dan Lea, Claire Lévy, Tomas Lovato, Nicolas Martin, Sébastien Masson, Silvia Mocavero, Julien Paul, Clément Rousset, Dave Storkey, Andrea Storto, and Martin Vancoppenolle. NEMO ocean engine. *Notes du Pôle de modélisation de l'Institut Pierre-Simon Laplace (IPSL)*, 2017. doi: 10.5281/ZENODO.1472492.

Marina Lévy, Audrey Estublier, and Gurvan Madec. Choice of an advection scheme for biogeochemical models. *Geophysical Research Letters*, 28(1):3725–3728, 2001. doi: 10.1029/2001GL012947.

Marina Lévy, D Iovino, Laure Resplandy, Patrice Klein, Gurvan Madec, Anne-Marie Treguier, Sebastien Masson, and Taro Takahashi. Large-scale impacts of submesoscale dynamics on phytoplankton: Local and remote effects. *Ocean Modelling*, 43–44:77–93, 2012. doi: 10.1016/j.ocemod.2011.12.003.

Marina Lévy, A S Krémeur, and Laurent Mémery. Description of the LOBSTER biogeochemical model implemented in the OPA system. Technical report, Laboratoire d'Océanographie Dynamique et de Climatologie - IPSL, 2005.

Rik Wanninkhof. Relationship between wind speed and gas exchange over the ocean. *Journal of Geophysical Research: Oceans*, 97(C5):7373–7382, 1992. doi: 10.1029/92JC00188.

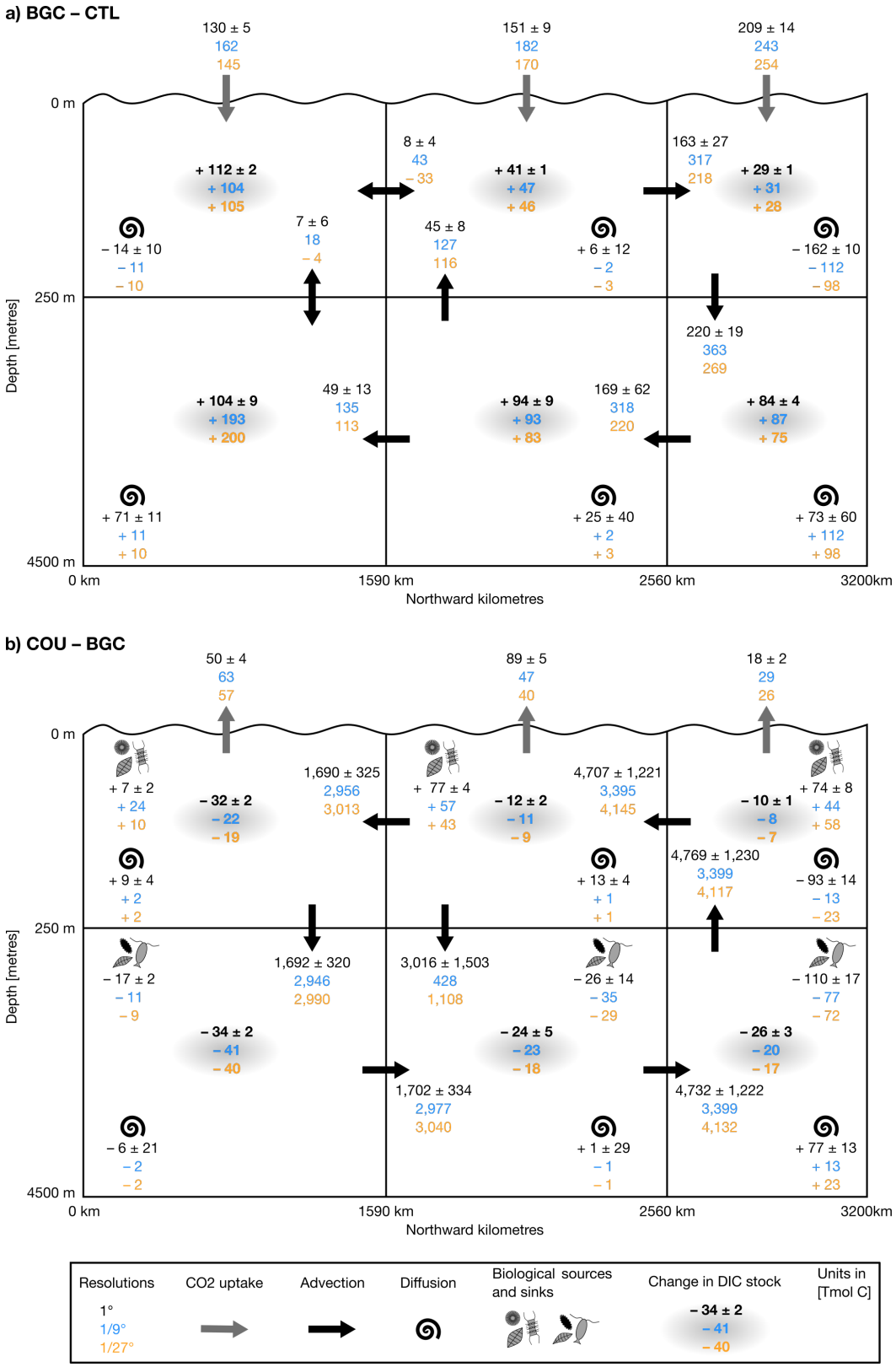

Figure S1. Differences in dissolved inorganic carbon (DIC) budgets (integrated over space and time) in the upper and lower ocean (resp. above and below 250 meters depth) for the three resolutions. a) Differences between the BGC and CTL simulations. b) Differences between the COU and BGC simulations. Bold numbers stand for difference in DIC stocks' change. Thin number for differences in CO_2 uptake, physical transport (advection, diffusion) and the biological sources and sinks. For CO_2 uptake, the arrows' direction indicate absorption or outgassing. For advection, arrows indicate the fluxes' direction. A double arrow indicate the flux is either in one direction or another, depending on resolution. At coarse resolution, the term diffusion combines vertical and isopycnal mixing, making it impossible to isolate bottom-up from north-south. However, finer resolution simulations do not include isopycnal mixing, DIC loss at the surface is thus transported to depth. The 1° resolution numbers are the average of the five 1° configurations ±1 inter-model standard deviation.

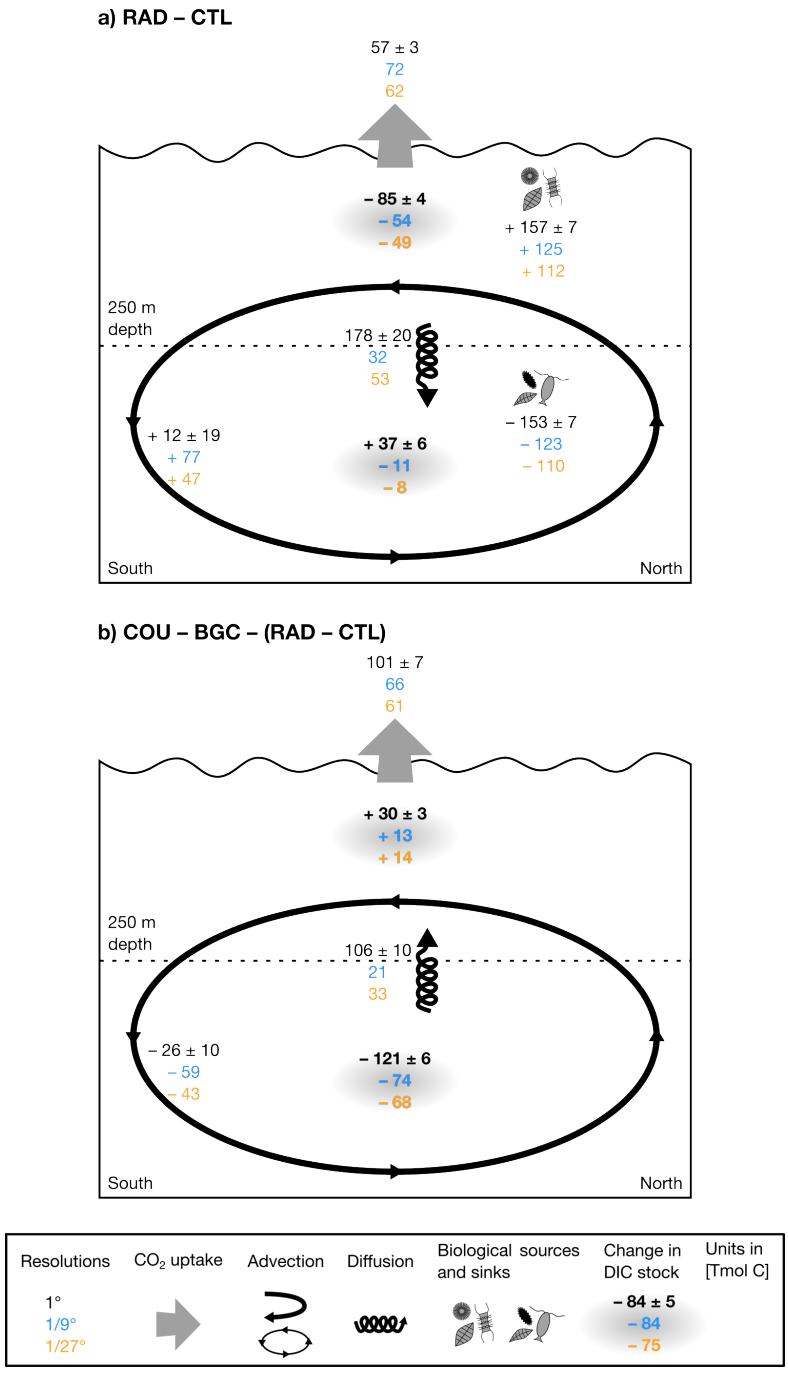

Figure S2. Same as Fig. 4 of the paper but a) for the differences between the RAD and CTL simulation and b) for the differences between the COU and BGC simulation minus the differences between the RAD and CTL simulations. In other words, a) shows the impact of the warming on the "natural" DIC budget, while b) shows the impact of the warming on the anthropogenic DIC budget.

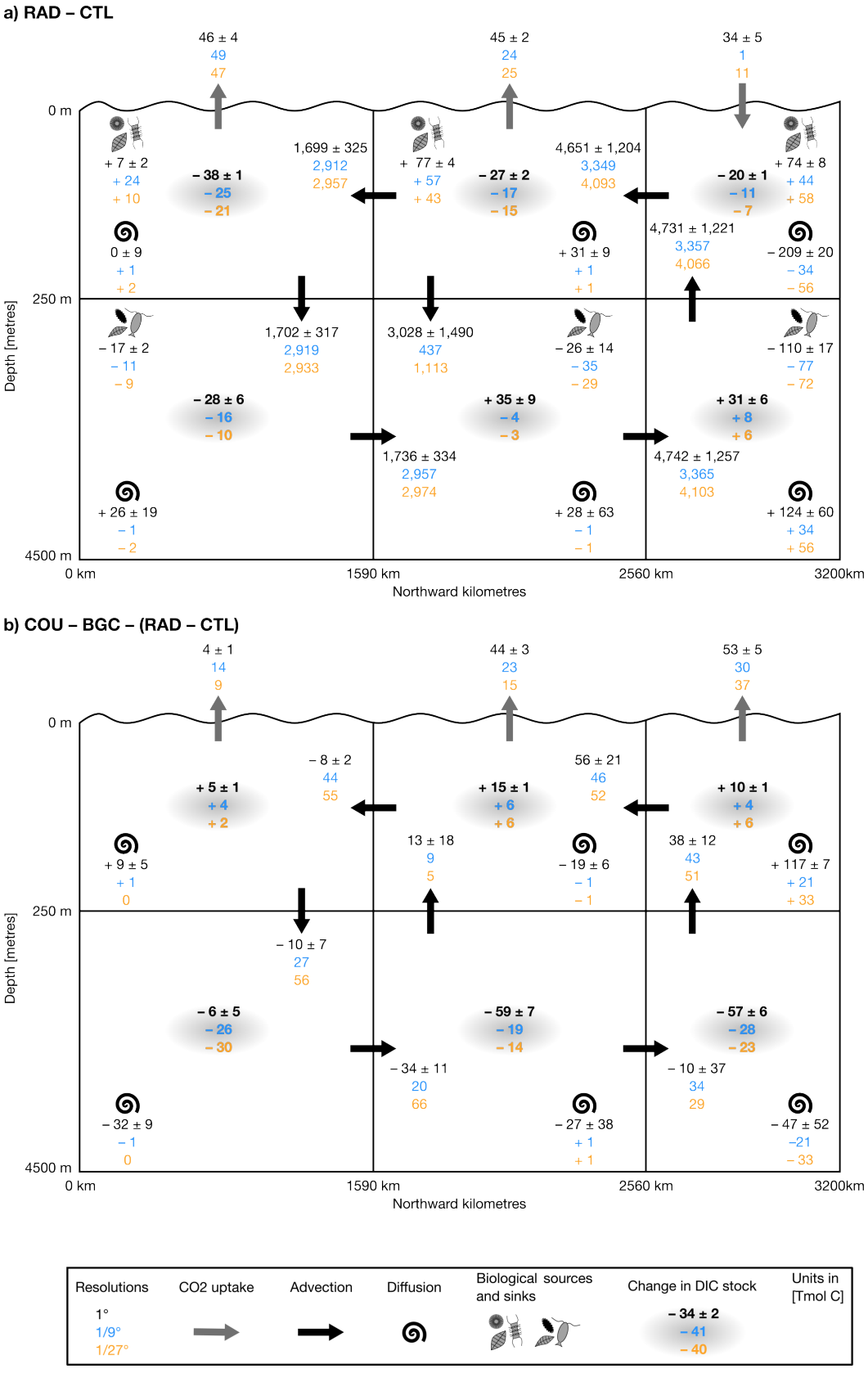

Figure S3. Same as Fig. S1 but a) for the differences between the RAD and CTL simulation and b) for the differences between the COU and BGC simulation minus the differences between the RAD and CTL simulations. In other words, a) shows the impact of the warming on the "natural" DIC budget, while b) shows the impact of the warming on the anthropogenic DIC budget.

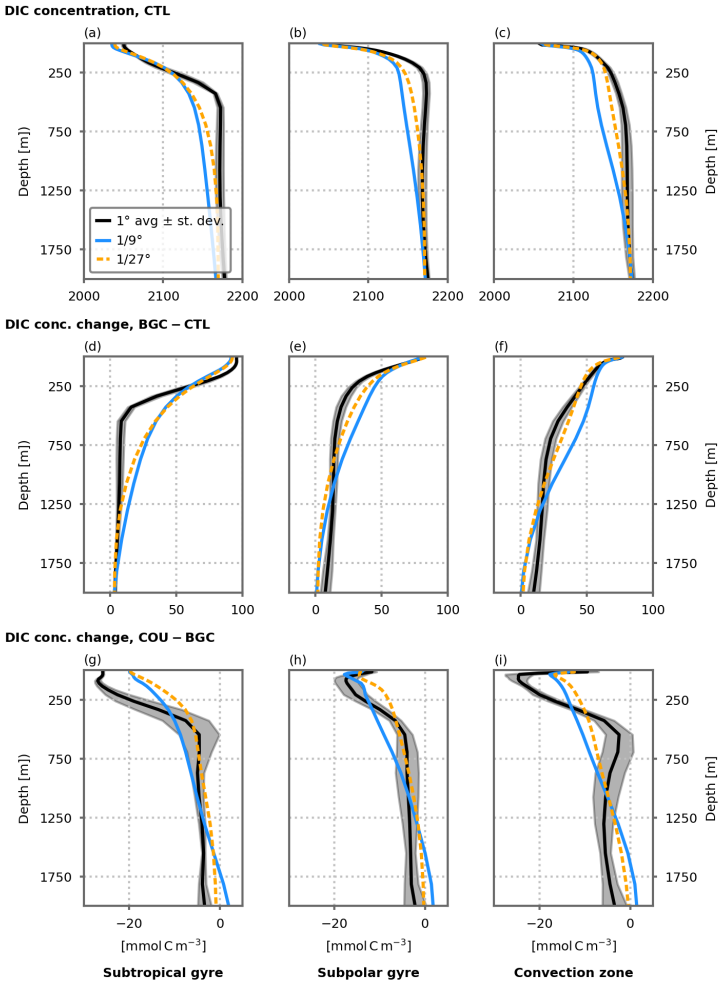

Figure S4. Dissolved inorganic carbon concentration (DIC, [mmol C m^{-3}]) vertical profiles spatially averaged over the subtropical gyre (0 to 1590 km northward), the subpolar gyre (1590 to 2560 km northward) and the convection zone (2560 to 3180 km northward), for the three resolutions. **(a, b, c)** DIC profiles in the CTL simulation. Change in DIC between **(d, e, f)** the BGC and CTL simulations and between **(g, h, i)** the COU and BGC simulations. All profiles are averages on the 10 last years of the simulations. The 1° resolution profiles shows the average of the five 1° configurations. Shading indicates ± 1 inter-model standard deviation.